REPRINT

Critical Reviews of
Optical Science
and Technology

Volume CR72

Overview of Variable Angle Spectroscopic Ellipsometry (VASE), Part II: Advanced Applications

from

Optical Metrology

Proceedings of a conference held

18-19 July 1999

Denver, Colorado

Overview of Variable Angle Spectroscopic Ellipsometry (VASE), Part II: Advanced Applications

Blaine Johs*, John A. Woollam, Craig M. Herzinger, James Hilfiker, Ron Synowicki, and Corey L. Bungay

J.A. Woollam Co., Inc., 645 'M' St. #102, Lincoln, NE 68508

ABSTRACT

A preceding companion paper provides a general introduction to Variable Angle Spectroscopic Ellipsometry (VASE), and also describes many typical applications of the technique. In this paper, more advanced VASE applications are discussed. These applications rely on recent advances in ellipsometric hardware, which allow extremely accurate ellipsometric data to be acquired over a broad spectral range, from the IR to VUV. This instrumentation can also quantitatively measure the optical response of non-isotropic samples. Advanced data analysis techniques are also presented.

Keywords: ellipsometry, advanced instrumentation, parametric models, multi-sample analysis, depolarization, anisotropy, Mueller matrix.

1. ADVANCED INSTRUMENTATION

One of the principal advantages of the ellipsometric technique is its potential for highly *precise* and *accurate* measurements. As ellipsometry measures a ratio quantity (Equation 1), the measurement is potentially more precise and accurate than a traditional intensity reflectance or transmission measurement (the precision and accuracy of intensity-based optical measurements can be hindered by baseline intensity drifts, difficulties in reproducibly collecting all of the measurement beam, and imperfect reference samples). On the other hand, since ellipsometry is a polarization-based measurement, relatively complex optical instrumentation is required (as compared to a simple intensity measurement; see Figure 1), and acquiring highly *accurate* ellipsometric data over wide spectral and angle ranges is not trivial.

Definition of ellipsometric parameters $\mathbf{Y}$ and $\mathbf{D}$:
(r_p and r_s are the complex Fresnel reflectivities for p- and s-polarized light)

$$\tan(\Psi)\cdot e^{i\Delta} = \frac{r_p}{r_s} \qquad (1)$$

When constructing a Variable Angle Spectroscopic Ellipsometer (VASE) system, ideal optical elements, namely polarizers and compensators, are desirable. An ideal optical

* Correspondence: Email: bjohs@jawoollam.com; www.jawoollam.com;
Telephone: 402-477-7501; FAX: 402-477-8214

element should impart a well defined polarization state to the probe beam over the spectral range of the instrument, and have minimal angular alignment sensitivity. Imperfect optical elements can also be utilized in ellipsometric instrumentation (and in fact they are an unfortunate necessity in some spectral ranges and instrument designs), but the non-idealities must be accurately characterized and accounted for in the data acquisition scheme to ensure accurate ellipsometric data. Furthermore, it is also necessary to accurately calibrate the ellipsometer system to determine the azimuthal orientation of the optical elements with respect to the sample plane of incidence. While a comprehensive discussion is beyond the scope of this article, numerous references[1,2,46] provide excellent overviews of traditional ellipsometric instrumentation and calibration procedures. In this section, recent state-of-the-art ellipsometric instrumentation which provides extremely accurate spectroscopic data is described, along with applications which exploit this advanced capability.

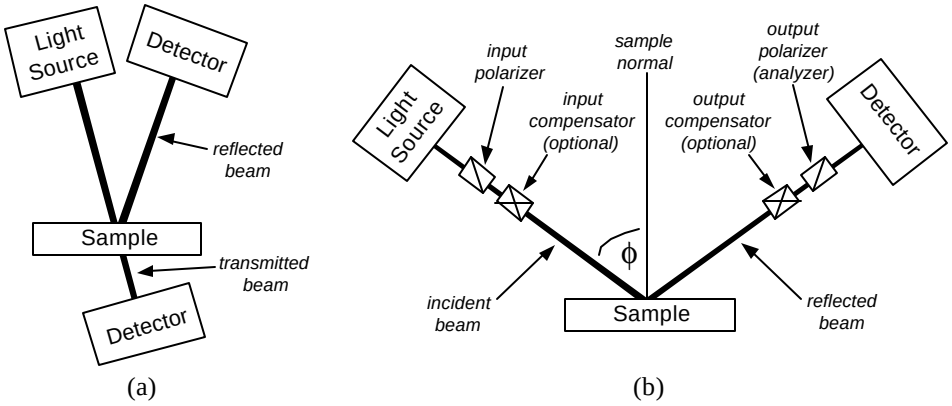

Figure 1. Basic components required for typical optical measurements: (a) near normal incidence intensity reflection and transmission instrumentation, (b) ellipsometric instrumentation for measurement at oblique angle of incidence 'ϕ'; the optical elements (polarizers and optional compensators) can be fixed, adjustable, continuously rotating, or electrically modulated depending on the particular ellipsometer configuration.

1.1. Compensator-based ellipsometer designs

The Rotating Analyzer Ellipsometer (RAE) configuration (and its counterpart, the Rotating Polarizer Ellipsometer (RPE) configuration) is commonly employed in spectroscopic ellipsometry systems. This relatively simple ellipsometer configuration requires only two polarizers, and since essentially ideal crystal polarizers are readily available, it is reasonably straight forward to build a high accuracy spectroscopic RAE or RPE system[2] which operates in the UV-VIS-NIR spectral range (190 – 1700 nm). However, there are well know limitations to this simple spectroscopic ellipsometer configuration[3]: 1) the 'handedness' of the ellipsometric Δ parameter can not be uniquely determined (Δ can range from 0 – 360°, but for Δ>180°, an RAE or RPE system will report $\Delta_{RAE} = 360° - \Delta_{actual}$), and 2) the precision and accuracy of the RAE or RPE measured Δ value is poor when Δ is near 0° or 180°. These limitations may be inconsequential for many applications, but for some samples (very thin dielectric films on glass, for example), very accurate measurements of Δ are required for adequate characterization of the sample.

Other ellipsometer configurations may not suffer from the aforementioned 'Δ' limitations, but they incur other tradeoffs. Null ellipsometer systems, for example, measure Ψ and Δ with high precision and accuracy over the entire measurement range; however, for various reasons, the null configuration is not generally employed in spectroscopic systems. Phase modulation ellipsometer (PME) systems measure Δ accurately over the full 0 – 360° range, but suffer from Ψ accuracy problems when Ψ is near 0° or 45°, depending on the particular instrument configuration[4] (this limitation can be overcome by the additional complexity of a dual channel detection system[5]). The photoelastic modulator used in PME ellipsometer systems are inherently chromatic optical elements, and the drive voltage must be accurately adjusted at each wavelength during a spectroscopic scan. Furthermore, due to the high modulation frequency, it is not possible to construct a PME system which simultaneously acquires spectroscopic ellipsometric data (implementing true parallel signal acquisition and readout) with existing diode array spectrometer technology.

1.1.1. Rotating Analyzer Ellipsometer (RAE) with Adjustable Retarder

In theory, the RAE and RPE 'Δ' measurement limitations can be eliminated by simply adding a compensator to the beam path (either before or after the sample). However, this is more challenging than it sounds, for several reasons: 1) a perfectly ideal spectroscopic compensator element does not exist, 2) compensator elements which can be used spectroscopically (such as Fresnel Rhombs) are only pseudo-achromatic, bulky, and difficult to align, and 3) if the retardance of the compensator is not meticulously calibrated (throughout the entire spectral range), or if the compensator is not properly aligned, the accuracy of the ellipsometric data will be degraded (instead of enhanced) by the introduction of the compensator element.

In spite of these challenges, one commercially available ellipsometer system does successfully integrate a compensating element with a high accuracy RAE[7]. In this system, a computer controlled MgF_2 Berek waveplate is used to accurately introduce retardance into the beam path[8]. Since the retarder is under computer control, it is possible to generate appropriate retardance values (0 – 90°) over a broad (150 – 1700 nm) spectral range. Figures 2 - 4 show examples of variable angle and spectroscopic ellipsometric data which were acquired with such a system. In these examples, it is the accurate measurement of the ellipsometric Δ parameter near 0° and 180° which enables a determination of the thickness and index of a dielectric film deposited on a polycarbonate substrate, and the optical constants and surface roughness layer on a glass microscope slide. A depolarization measurement of the glass microscope slide is also shown in Figure 4. This is another capability provided by the addition of the adjustable retarder, and is discussed in more detail in section 3.2.

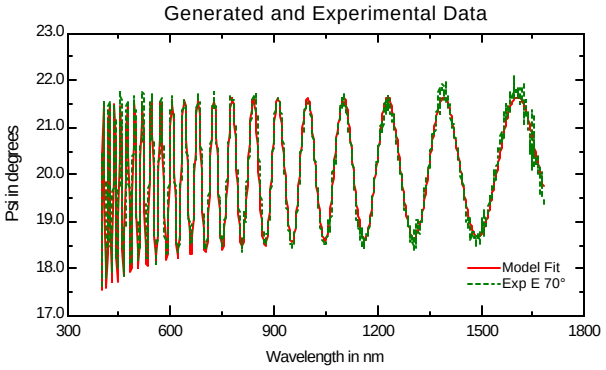

(a)

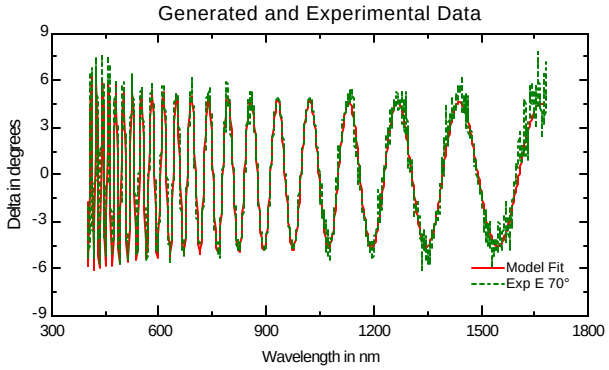

(b)

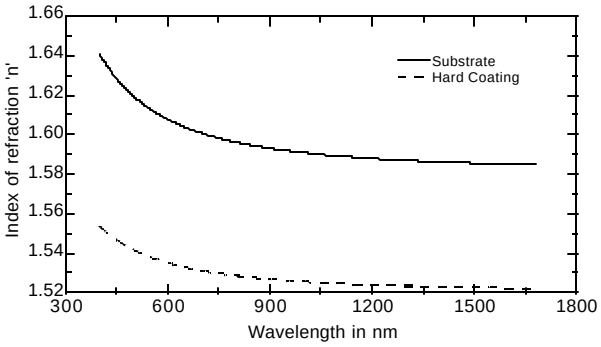

(c)

Figure 2. Ellipsometric Ψ (a) and Δ (b) data acquired with a retarder-equipped RAE system[7] on a polycarbonate lens with a thick (4.35μm) hard coating. Accurate measurement of the period and amplitude of oscillations in both Ψ and Δ enabled accurate determination of the film thickness and optical constants (c).

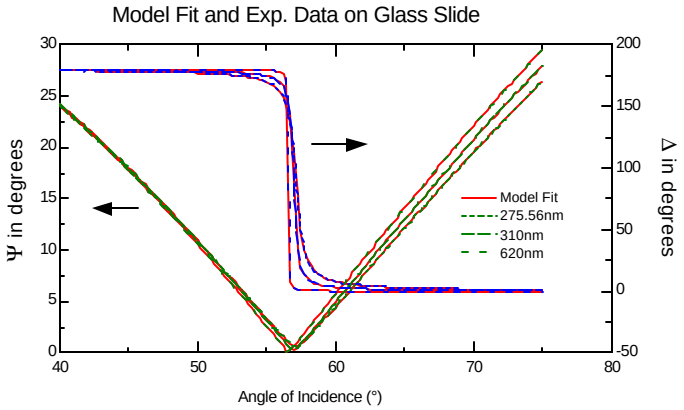

Figure 3. Accurate measurement of variable angle ellipsometric data near the Brewster angle on a glass microscope slide, using an RAE system with an adjustable retarder[7]. To achieve the near perfect data fits shown in the graph, it was necessary to add 23Å of surface roughness to the front and back surfaces of the glass in the optical model. The more rounded Δ curves correspond to the shorter wavelength data, where the glass is more absorbing.

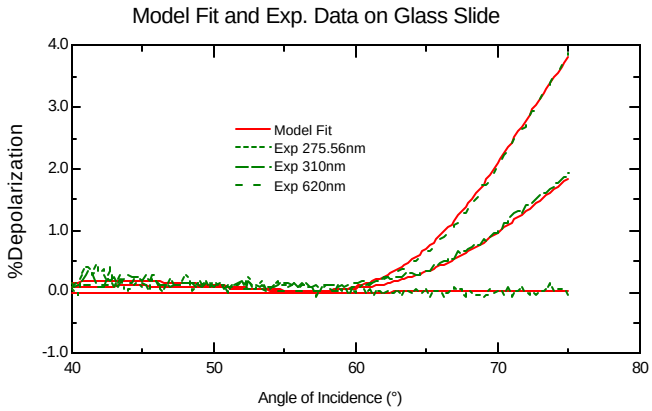

Figure 4. Depolarization measurement of a glass microscope slide with a retarder-equipped RAE system[7]. The depolarization is caused by the backside reflection of the slide; as the glass becomes opaque at shorter wavelengths, the depolarization goes to zero.

1.1.2. Rotating Compensator Ellipsometer (RCE) Configuration

Another approach to introducing a compensator into the ellipsometer beam path is to implement the Rotating Compensator Ellipsometer (RCE) configuration. There are many advantages to the RCE configuration, including[9]: accurate measurement of the ellipsometric Ψ and Δ parameters over the complete measurement range (Ψ=0-90°, Δ=0-360°), no residual input or output polarization sensitivity (due to a fixed polarizer on input, and a fixed analyzer on the output), and the capability to directly measure depolarization effects. However, only recently have Spectroscopic RCE systems been constructed[10-14]. The prior lack of spectroscopic RCE systems, in spite of the well known advantages to this configuration, was mainly due to the perceived difficulty of constructing a mechanically rotatable compensator element which behaves ideally (retardance ≈90°) over a wide spectral range. Recently, this challenge has been

successfully addressed in a number of ways: 1) a special rhomb-like prism retarder has been used to implement a Fourier Transform Infra Red (FTIR) RCE system[15](data from which will be shown in the IR-VASE section of this paper), 2) a realization that ellipsometric data can still be acquired (albeit with reduced Δ measurement capability) even as the retardance of the compensator passes through 180° in part of the spectrum[11] (which is inevitable when using standard waveplates for compensator elements, as their retardance exhibits a $1/\lambda$ dependence), and 3) development of multi-element, pseudo-achromatic compensators coupled with a rigorous calibration methodology[16]. A commercially available spectroscopic RCE instrument is based on approach #3[14]. This instrument also employs a diode array spectrometer (Diode Array Rotating Compensator Ellipsometer, or DARCE), such that simultaneous acquisition of spectroscopic ellipsometric data is possible[17]. In addition, by switching the light source and/or diode array detector, it is possible to cover a variety of spectral ranges, from the DUV (190 nm) to the NIR (1700 nm).

Figure 5 shows ellipsometric data which was acquired on an ITO film with a VIS-NIR DARCE system[14]. In this system, a quartz tungsten halogen (QTH) light source was directly coupled into the DARCE input optics, and a bifurcated collection fiber split the output beam into two diode array spectrometers: a Si-based array covering the 400-1000nm spectral range, and an InGaAs-based array covering the 1000-1700nm spectral range. Data is simultaneously acquired on both diode arrays, such that a 1-2 second acquisition time results in ellipsometric data covering the 400-1700nm spectral range with excellent precision and accuracy. Characterization of flat panel display materials, such as Indium Tin Oxide (ITO) and thick amorphous Si films, is greatly enhanced by ellipsometric measurements in this NIR spectral range[18]. Likewise, the communications industry which utilizes optics and coatings that operate near 1.3 and 1.5 µm would greatly benefit from fast spectroscopic ellipsometric material characterization in this VIS-NIR spectral range.

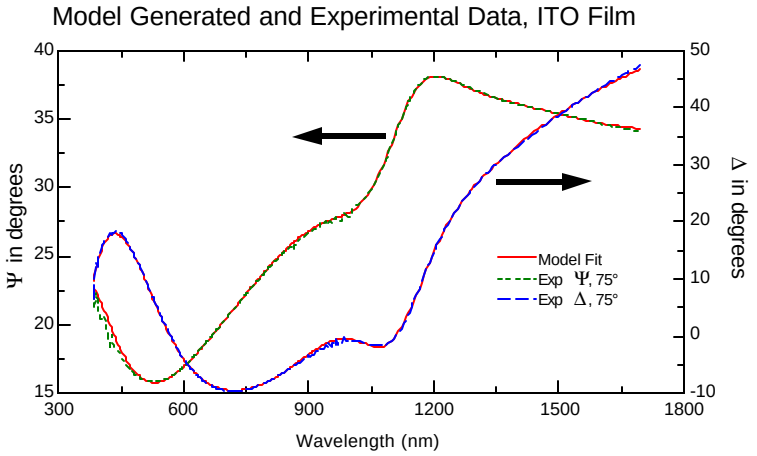

(a)

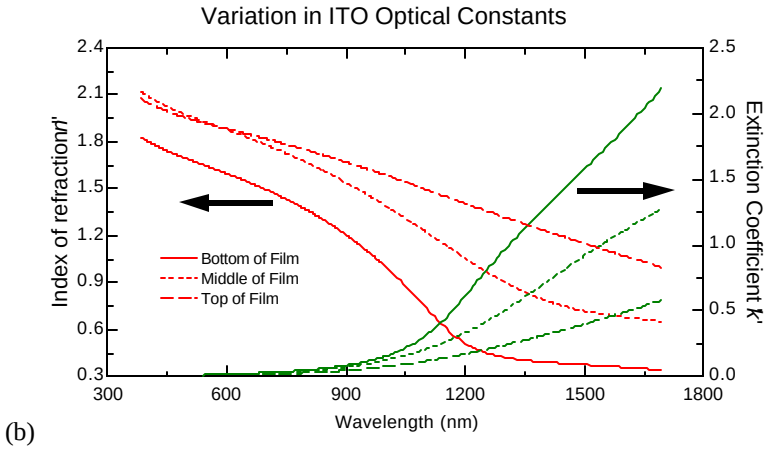

(b)

Figure 5. (a) DARCE data acquired on an Indium Tin Oxide (ITO) coating on glass sample; note the accurate 'Δ' measurements near 0°. (b) ITO optical constants resulting from analysis of the data shown in (a), using a graded optical model; note the variation in free-carrier optical absorption in the NIR spectral range (1000-1700 nm). The optical absorption is directly related to the electrical conductivity of the film, which is critical for flat panel display applications and highly dependent on the annealing process.

1.2. Verification of Ellipsometric Accuracy: Straight-Through (Air) Measurements

Verifying the accuracy of an ellipsometric system is not a simple matter. Reference standards have been proposed[19], however, preparing a sample which exhibits reproducible optical properties to the level of precision offered by a typical Spectroscopic Ellipsometer system is not feasible in most laboratories, let alone a manufacturing environment. Reference SiO_2 on Si wafers are available from NIST and other companies; however, the precision of most ellipsometer systems is still much better than the tolerance of the reference standards (and the reference standards may also change over time). Even the optical constants and model for SiO_2 on Si structures, which is arguably the most well studied material system by ellipsometry, are still a subject of discussion in the literature[20,21].

The only material for which the ellipsometric parameters are absolutely known is 'Air': an ellipsometric measurement in the straight-through configuration should by definition return Ψ=45° and Δ=0°. A straight-through measurement is a 'necessary but not sufficient' accuracy criteria for an ellipsometer system: accurately measuring Ψ=45° and Δ=0° in the straight-through configuration does not guarantee that the ellipsometer will also measure accurate ellipsometric data on general samples, but any deviations from ideal behavior observed in straight-through measurements certainly imply that measurement errors will be present in ellipsometric data acquired on real samples as well.

Figure 6 shows straight-through measurement data which was acquired using commercially available Spectroscopic Ellipsometer systems utilizing compensators[7,13,14] over a broad spectral range (190nm - 40μm). Note that the deviations in the measured data from the ideal values is much less than 0.1° over most of the entire range. As some papers[22] report straight-through tan(Ψ) and cos(Δ) measurements (which should both be

exactly 1.0), Figure 7 plots the data from Figure 6 transformed into tan(Ψ) and cos(Δ). Note that for a compensator-based ellipsometer system which can accurately measure Δ near 0°, the cos(Δ) parameter becomes ridiculously close to 1.0.

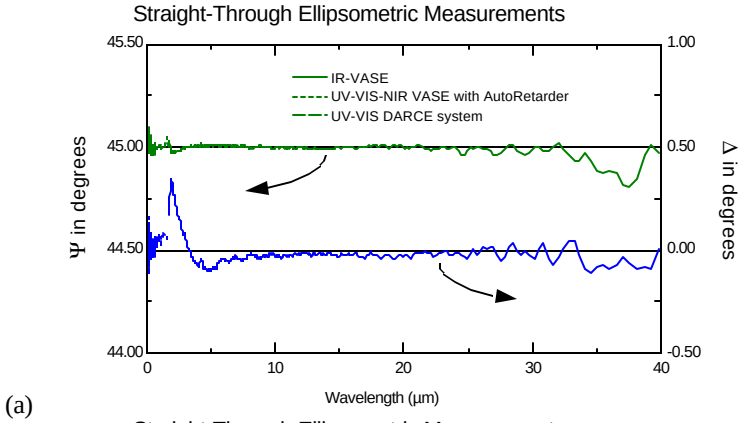

(a)

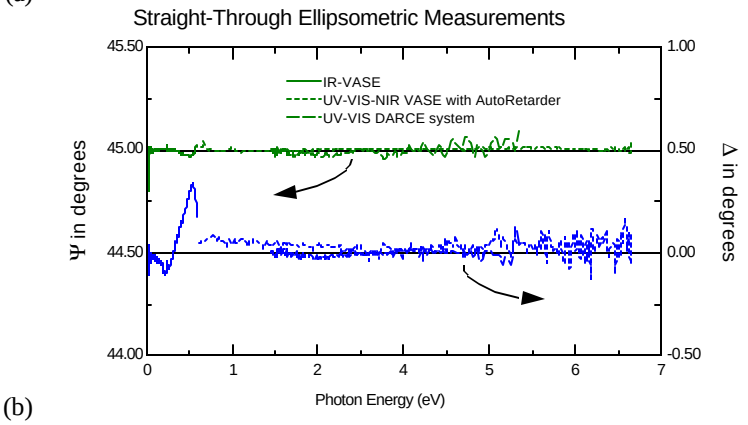

(b)

Figure 6. Straight-through ellipsometric measurements of 'air' performed on commercially available Spectroscopic Ellipsometer systems [7,13,14], plotted in wavelength (a), and photon energy (b). For an ideal system, Ψ=45° and Δ=0° for this measurement.

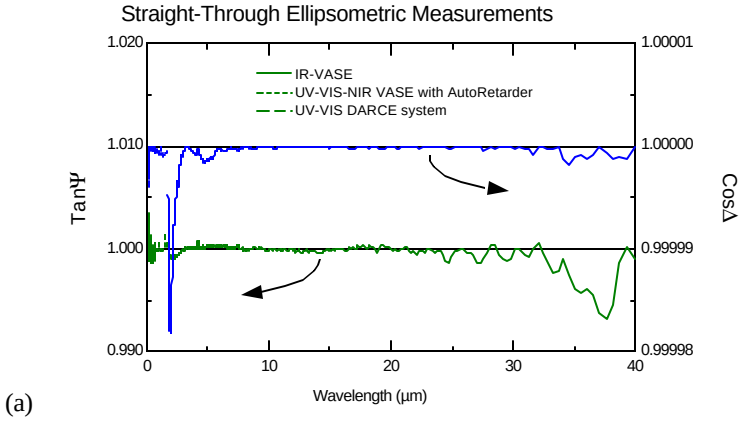

(a)

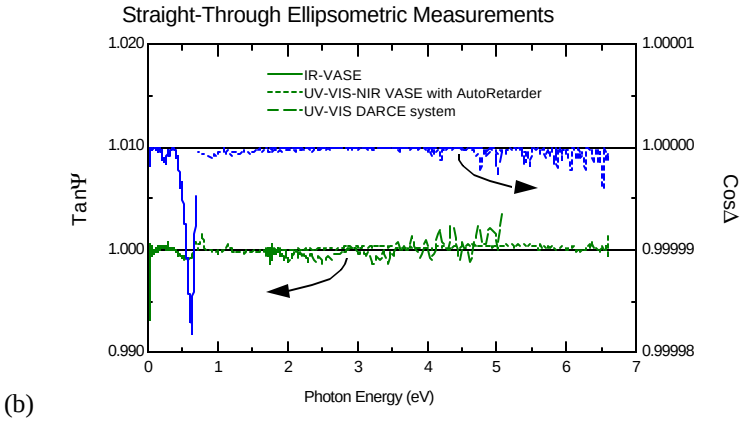

(b)

Figure 7. Straight-through ellipsometric measurements of 'air' performed on commercially available Spectroscopic Ellipsometer systems [7,13,14], transformed into tan(Ψ)/cos(Δ) notation and plotted in wavelength (a), and photon energy (b). For an ideal system, tan(Ψ)=cos(Δ)=1.0 for this measurement.

2. ADVANCED DATA ANALYSIS TECHNIQUES

When analyzing ellipsometric data from a sample which consists of materials with well known optical constants, it is very straight forward to build an optical model for the sample, and perform regression analysis of the data to extract layer thicknesses and surface/interfacial roughness[23]. However, for many (if not most) materials, optical constants are not well known or may vary, depending on the material preparation method (the term 'optical *constant*' is somewhat of a misnomer). Therefore, extracting accurate material optical constants is an important component of ellipsometric data analysis. For ideal bulk or single layer structures, it is possible to directly invert optical constants 'n' and 'k' from the ellipsometric parameters Ψ and Δ. For more complicated structures which include multiple layers, non-ideal interfaces, or gradients in the film optical properties, advanced data analysis techniques are required to simultaneously and uniquely extract optical constants (sometimes of multiple materials) and structural information (film thicknesses, surface/interfacial roughness, grading profile) from the VASE data.

2.1. Optical Constant Parameterization by GBPS

VASE measurements are typically performed over a wide spectral range, and for quantitative analysis of the data, it is necessary to specify material optical constants over the complete spectral range of the data. Of course, it is always possible to describe the dispersion in optical constants by a tabulated list of 'n' and 'k' values (or equivalently, the real and imaginary parts of the dielectric function, ε_1 and ε_2) at discrete wavelengths (and interpolating within the table as necessary). However, such a tabulated list requires large number of parameters (2X the number of wavelengths in the data set), and does not enforce any Kramers-Kronig (K-K) consistency between the real and imaginary parts of the dielectric function[24]. A parametric dispersion model enables the calculation of

material optical constants as a function of wavelength, using a much smaller set of free parameters. The literature contains many parametric dispersion models which are useful in the analysis of ellipsometric data, including Cauchy, Sellmeier, Harmonic Oscillators[25], Tauc-Lorentz[26], and others[27-29]. For example, the Cauchy dispersion parameterization is shown in Equation (2). Many of the dispersion models are appropriate for only specific types of materials, for example, the Cauchy model is valid only for transparent materials, and the Tauc-Lorentz[26] works best for amorphous materials. In this section, a general Guassian-Broadened Polynomial Superposition (GBPS) parametric dispersion model is described, which can be broadly applied to most materials including crystalline and amorphous semiconductors, metals, and organics.

$$n(\lambda) = A + \frac{B}{\lambda^2} + \frac{C}{\lambda^4} \ , \quad k(\lambda) = 0 \tag{2}$$

The details of the GBPS parametric dispersion model can be found elsewhere[30], however, the model is fundamentally constructed by a superposition of piece-wise continuous polynomials which are numerically convolved with Gaussian oscillator lineshapes (see Figure 8). While this model does not attempt to directly capture the underlying physics of the material dielectric function, it does have a number of advantages when compared to other dispersion models: 1) the resulting dielectric function is K-K consistent, 2) the use of 'true' Gaussian broadening allows for complete transparency below the fundamental band gap, 3) it is flexible enough to represent the subtle nuances in dielectric function spectra which are often not adequately described by first principles physics-based models, 4) ε_2 is strictly positive (absorbing) for all positive frequencies, and 5) the parameterization is stable and robust, such that direct regression analysis of ellipsometric data is possible, and parameterized composition and temperature dependent dielectric function spectra can be readily constructed[31].

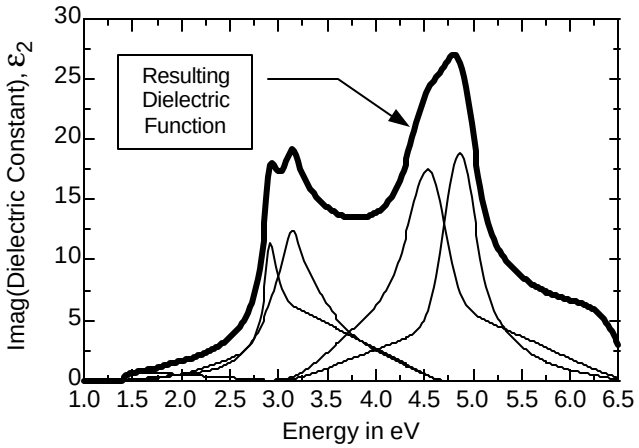

Figure 8. Construction of a GBPS parametric dielectric function representation by a summation of Gaussian-broadened polynomial segments (the resulting dielectric function in this figure is for GaAs, and is valid for E<6eV).

To illustrate the ellipsometric data analysis capabilities provided by the GBPS parametric model, consider the following examples. Figure 9 shows the dielectric function of crystalline GaAs, which is accurately represented by the GBPS model with only 23 free parameters over the entire spectral range: below, at, and above the fundamental band gap. Figure 10 shows VASE data and extracted optical constants for a diamond-like carbon (DLC) film deposited on Si. To achieve this excellent level of agreement between the experimental and model fit data, only 5 fitting parameters were used: the DLC film thickness plus 4 parameters of the GBPS parameterized DLC optical constants. The ITO optical constants shown in Figure 5(b) were also parameterized by the GBPS model, enabling a simultaneous determination of the film optical constants, layer thickness, and grading profile.

In summary, optical constant parameterization is a powerful technique for analyzing VASE data acquired on complex samples. By greatly reducing the number of parameters required to model the dispersion, material optical constants and structural information about the sample (such as layer thicknesses) can be simultaneously and uniquely determined. Utilizing optical constant parameterization in a multi-sample analysis (described in the next section) and over wide spectral ranges (also described in a subsequent section) further enhances the power of the technique. The GBPS model is a very general parametric dispersion model which can be applied to almost any material which exhibits optical absorption in the spectral range of the VASE measurement.

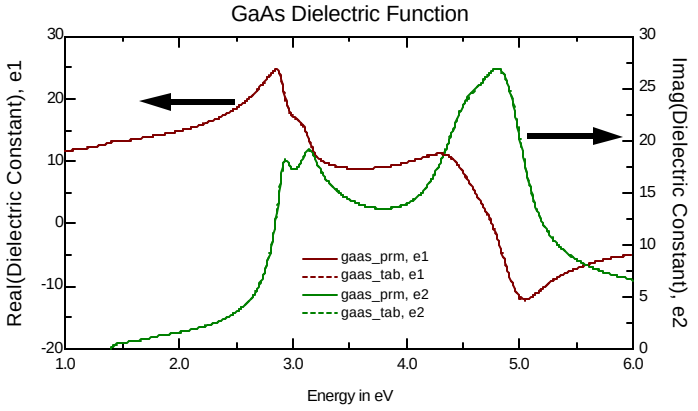

(a)

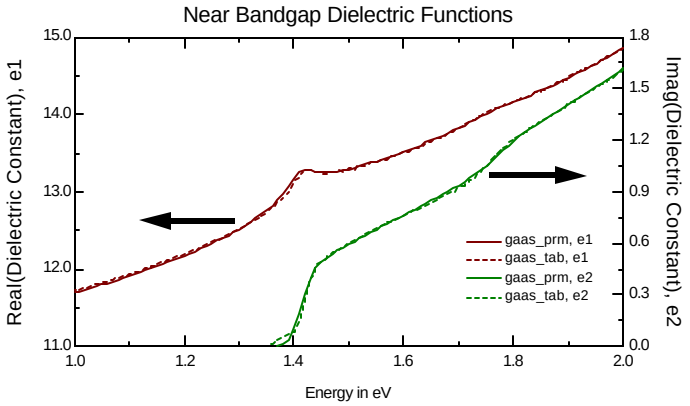

(b)

Figure 9. (a) Accurate parametric representation of the GaAs dielectric function over a wide spectral range; using the GBPS model with only 23 free parameters. (b) Blow-up of (a) comparing the tabulated values with the GBPS model near the GaAs fundamental band gap.

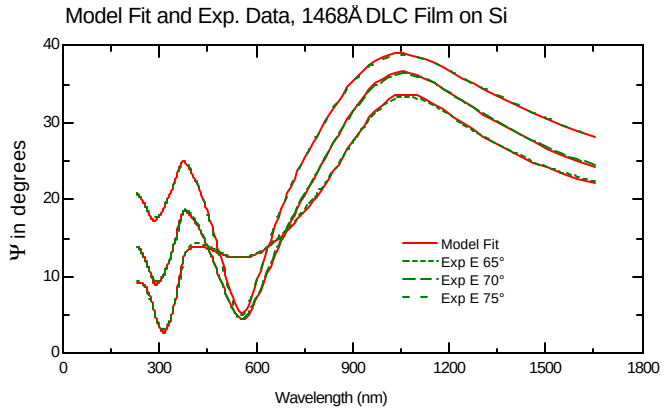

(a)

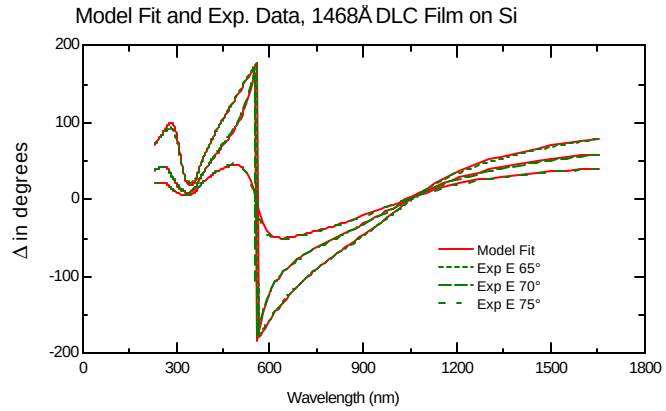

(b)

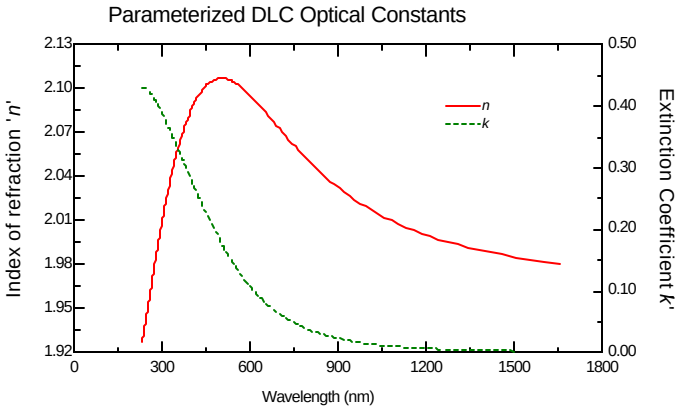

(c)

Figure 10. (a,b) Experimental VASE data and corresponding model fit data for a Diamond-like carbon (DLC) film deposited on Si; note the excellent model fits. (c) Optical constants extracted from the data in (a) and (b) using the GBPS parametric dielectric function model; only 4 adjustable parameters were required to describe the dispersion over the 230-1700nm spectral range.

2.2. Multi-Sample Analysis

If the optical constants for a given material are truly *constant*, then those same optical constants should accurately fit the VASE data acquired from any sample which includes the material. That is the premise behind the powerful multi-sample analysis technique. In this technique, VASE data from multiple samples are simultaneously included in the regression analysis, and a common set of optical constants is 'coupled' into the optical model used for each sample. By including samples with a range of layer thicknesses, the information content of the data set is greatly enhanced, enabling the simultaneous and accurate determination of all the layer thicknesses of the samples, and layer optical constants (sometimes for even more than one material). Each sample adds one additional thickness fit parameter to the analysis, but this is offset by the sample's VASE data, which may have been acquired over multiple angles and hundreds of wavelengths. The concept of simultaneously analyzing ellipsometric data from multiple samples has been routinely employed in the analysis of single wavelength ellipsometric data[32]. However, it seems to be under-utilized in VASE data analysis, possibly due to the added complication of handling multiple data sets in the optical modeling and regression software. The only fundamental requirement of the multi-sample technique is a systematic series of samples with material of uniform optical properties covering a range of layer thicknesses; this requirement can be readily achieved for many material systems.

The literature contains a number of good examples of multi-sample analysis of VASE data[33,34]. To illustrate this technique, we will present a multi-sample analysis consisting of SiO_2 on Si wafers, in which the Si and SiO_2 optical constants, along with SiO_2 and interfacial layer thicknesses, are simultaneously extracted. This analysis is based on the work of Herzinger[21]; in this example we have extended the spectral range of the ellipsometric measurements (and hence the optical constants) to 8.5 eV (see section 4.2 for a description of the VUV ellipsometer instrumentation). The four samples used for this example are described in Table I. Note that different angles, spectral ranges (covering NIR-VIS-UV-VUV), and resolutions were used for the ellipsometric data sets (higher resolution scans were used for the 1µm thick film to better resolve the

interference fringes). Since a parametric representation was used for the optical constants (the Si optical constants used a GBPS parameterization, and a two term Sellmeier dispersion function was used for SiO_2), it is not necessary that all data sets cover the same spectral range. To achieve the excellent model fits to the experimental data which are shown in Figures 11 – 14, an interfacial layer between the Si substrate and oxide film was required. The optical nature of this interface is thoroughly discussed elsewhere[21,52], and in this work we treated the interfacial layer in the same manner: the interfacial layer optical constants were assumed to be transparent with a higher index than the oxide film (the index offset was taken from Ref. 21), and they were constrained to follow the same dispersion as the oxide film. The results of the multi-sample analysis are shown in Table I (layer thicknesses) and Figures 15 and 16 (optical constants). The Si and SiO_2 optical constants are self-consistent (by virtue of the multi-sample analysis), and they were determined without any special sample preparation (such as stripping the oxide, which can add uncertainties to the data analysis[35,36].

Sample	Experimental Ellipsometric Data	Interface Thickness (Å)	SiO2 Thickness (Å)
nominal 250Å thermal oxide on Si	0.75 - 6.0 by 0.01 eV, at 70°, 75°, 80°	8.9±1.5	253.1±1.2
native oxide on Si	4.2 - 8.5 by 0.05 eV, at 75.5°	10.6±2.5	10.9±3.1
nominal 280Å thermal oxide on Si	4.2 - 8.25 by 0.05 eV, at 75.5°	8.9±1.9	270.6±1.7
nominal 1µm thermal oxide on Si	4.7- 8.25 by 0.02 eV, at 75.5°	37.0±2.3	10474±10

Table I. Description of samples and resulting layer thicknesses from a multi-sample VASE analysis of SiO_2 on Si wafers. The '±' values on the thickness values are the 90% statistical confidence limits reported by the regression analysis of the data.

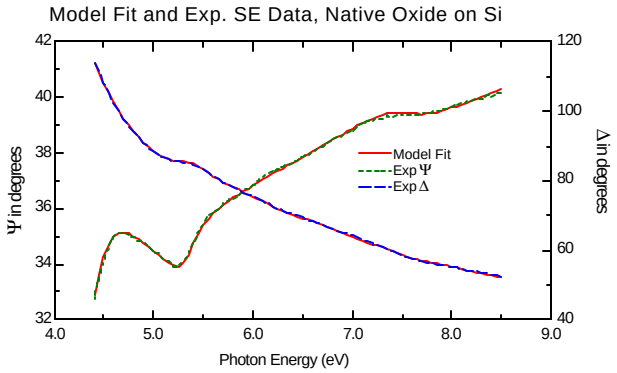

Figure 11. Model fit and experimental VUV spectroscopic ellipsometric data for the native oxide on Si sample which was part of a multi-sample analysis.

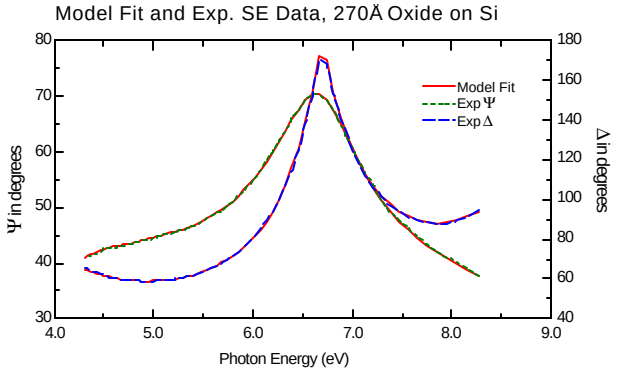

Figure 12. Model fit and experimental VUV spectroscopic ellipsometric data for the thermal oxide (nominally 270Å) on Si sample which was part of a multi-sample analysis.

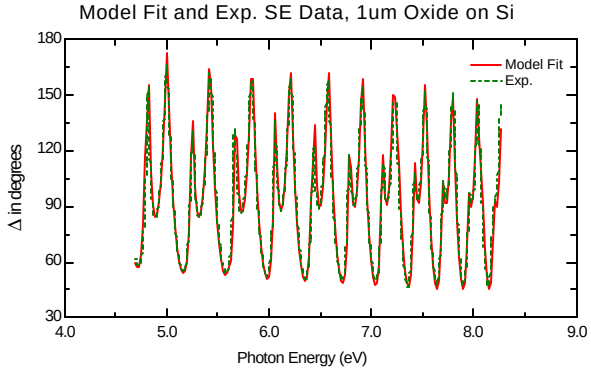

Figure 13. Model fit and experimental VUV spectroscopic ellipsometric data (only Δ is shown for clarity) from the thick thermal (nominally 1μm) oxide on Si sample which was part of a multi-sample analysis.

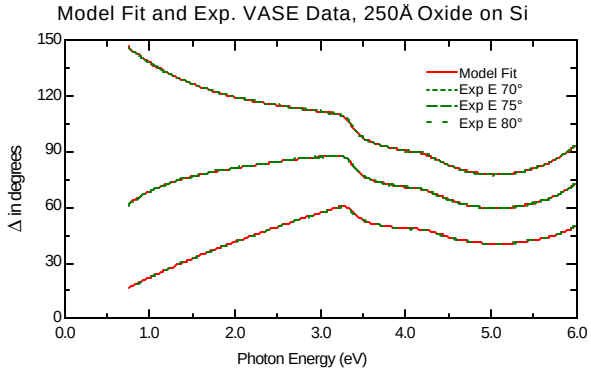

Figure 14. Model fit and experimental NIR-VIS-UV spectroscopic ellipsometric data (only Δ is shown for clarity) from the thermal oxide on Si sample which was part of a multi-sample analysis.

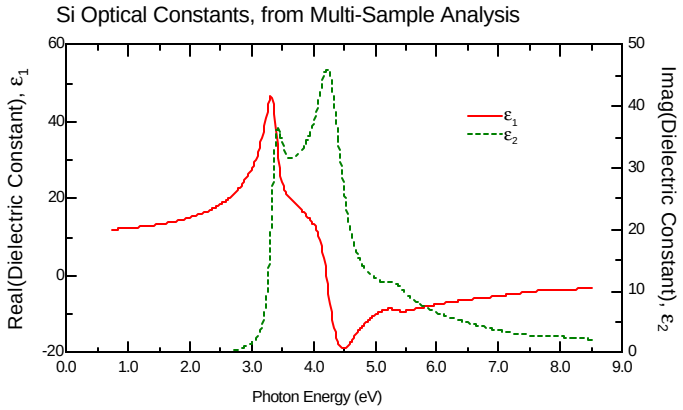

Figure 15. Si optical constants covering the NIR-VIS-UV-VUV spectral range (0.75 – 8.5 eV, or 146 – 1650 nm) extracted from a multi-sample VASE analysis of SiO_2 on Si wafers.

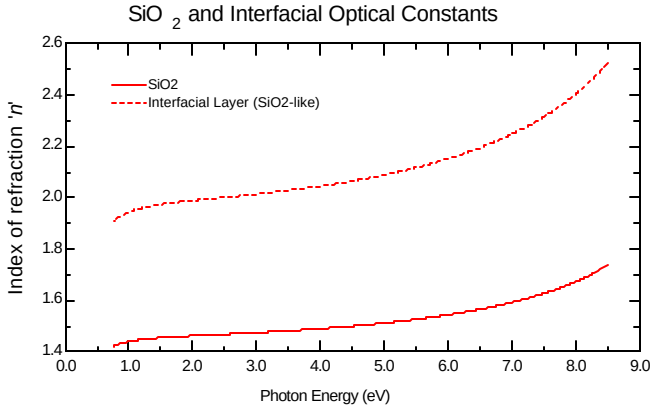

Figure 16. SiO_2 and Si/oxide interfacial optical constants covering the NIR-VIS-UV-VUV spectral range (0.75 – 8.5 eV, or 146 – 1650 nm) extracted from a multi-sample VASE analysis of SiO_2 on Si wafers.

3. BEYOND ISOTROPIC

Traditionally, most ellipsometric measurements have assumed an isotropic and non-depolarizing sample. While this assumption is indeed valid for most measurements, there are classes of samples which do exhibit anisotropic and/or depolarizing behavior. In these cases, it is not possible to adequately characterize the sample by a simple ellipsometric measurement of Ψ and Δ. While the literature has addressed the theory of non-isotropic ellipsometric measurements[37-40], recent advances in ellipsometric instrumentation[7,14,41,42] have made automated measurement of non-isotropic samples more practical, examples of which will be presented next.

3.1. Generalized Variable Angle Spectroscopic Ellipsometry (g-VASE)

The interaction of polarized light with an isotropic sample can be represented by the Jones matrix formalism shown in equation (3). The diagonal nature of the Jones matrix

in this equation implies no sample-induced coupling between the p- and s- polarized modes.

$$\begin{bmatrix} p_{out} \\ s_{out} \end{bmatrix} = \begin{bmatrix} r_p & 0 \\ 0 & r_s \end{bmatrix} \cdot \begin{bmatrix} p_{in} \\ s_{in} \end{bmatrix} \tag{3}$$

The Jones matrix for a *general* sample is not necessarily diagonal, as shown in equation (4). For such a sample, three ellipsometric ratios can be defined; one possible notation for the general ellipsometric parameters[43,44] is listed in Equations (5a-5c). For an isotropic sample, Aps=Asp=0, and AnE reduces to the standard ellipsometric ratio given in equation (1). The three generalized ellipsometric ratios can be experimentally measured with standard ellipsometric instrumentation, however, special data acquisition schemes (which can be implemented in software) are usually required.

$$\begin{bmatrix} p_{out} \\ s_{out} \end{bmatrix} = \begin{bmatrix} r_{pp} & r_{sp} \\ r_{ps} & r_{ss} \end{bmatrix} \cdot \begin{bmatrix} p_{in} \\ s_{in} \end{bmatrix} \tag{4}$$

$$AnE = \tan(\Psi) \cdot e^{i\Delta} = \frac{r_{pp}}{r_{ss}} \tag{5a}$$

$$Aps = \tan(\Psi_{ps}) \cdot e^{i\Delta_{ps}} = \frac{r_{ps}}{r_{pp}} \tag{5b}$$

$$Asp = \tan(\Psi_{sp}) \cdot e^{i\Delta_{sp}} = \frac{r_{sp}}{r_{ss}} \tag{5c}$$

3.1.1. g-VASE Measurements of Anisotropic Plastics

Transmission mode g-VASE data acquired on a ≈90 μm thick biaxially stretched plastic film (poly-ethyleneterephthalate, or PET) is shown in Figure 17. Note the incredible amount of structure in the plotted Ψ_{ps} quantity (which would be zero for an isotropic sample). This complex data set was also quantitatively analyzed (g-VASE data was calculated for the anisotropic optical model using a 4x4 matrix algorithm[45]) as evidenced by the data fits shown in Figure 18. The final result of the analysis was a determination of the three principal indices of refraction for the biaxial plastic (the index differences are plotted in Figure 19), which were found to be in excellent agreement with Abbe refractometer measurements, along with the azimuthal orientation of the film's optical axis. A detailed discussion of these results can be found in the literature[44].

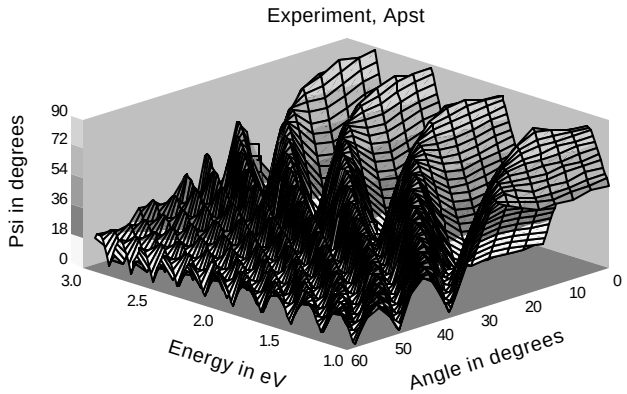

Figure 17. g-VASE data acquired on a biaxially stretched plastic film. The experimentally measured (in transmission) ellipsometric Ψ_{ps} value is plotted as a function of photon energy and angle of incidence.

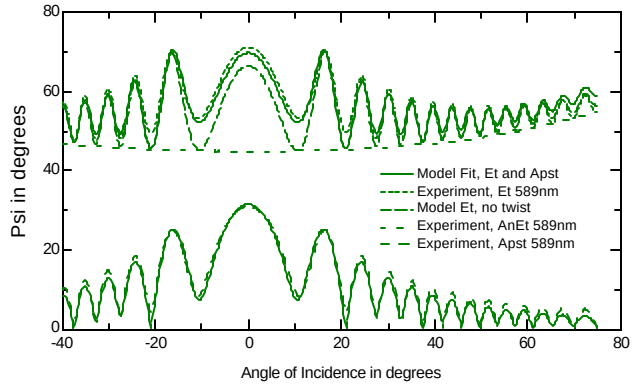

Figure 18. Quantitative analysis of g-VASE data acquired on a biaxially stretched plastic film, plotted at one wavelength vs. angle of incidence for clarity. The best model fit included a 'twist' in the orientation of the optical axis from the top to the bottom of the film.

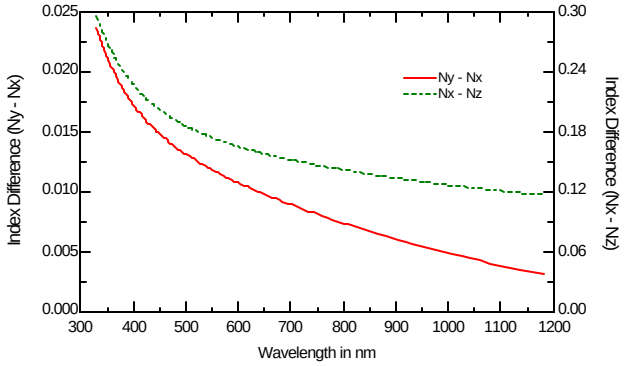

Figure 19. Difference of the principal indices of refraction, extracted from the analysis of the PET film g-VASE data shown in Figures 17 and 18.

3.1.2. Diode Array Rotating Compensator Ellipsometer g-SE Measurements

In addition to advantages discussed in section 1.1.2, the rotating compensator ellipsometer (RCE) configuration is also well suited for generalized ellipsometry measurements. Not only can the RCE accurately measure Δ over the full 0 – 360° range, it also measures Ψ accurately over the full 0 – 90° range (RAE systems also loose sensitivity when Ψ approaches 0° or 90°). The ability to accurately measure very small Ψ values is very useful when performing generalized ellipsometry measurements, as the 'off-diagonal' ellipsometric ratios A_{ps} and A_{sp} (and therefore Ψ_{ps} and Ψ_{sp}) are zero and near-zero, for isotropic and slightly anisotropic samples respectively. A Diode Array Rotating Compensator Ellipsometer (DARCE) system can rapidly perform generalized spectroscopic ellipsometer (g-SE) measurements by acquiring data sets at analyzer azimuths of 0°, 45°, and 90°, and algebraically transforming the three data sets into the notation shown in Equations (4-5). An example of DARCE g-SE measurements is shown in Figure 20. The acquisition of this data required only a few seconds; there should be many potential applications for the fast anisotropic material characterization capability provided by a DARCE g-SE measurements.

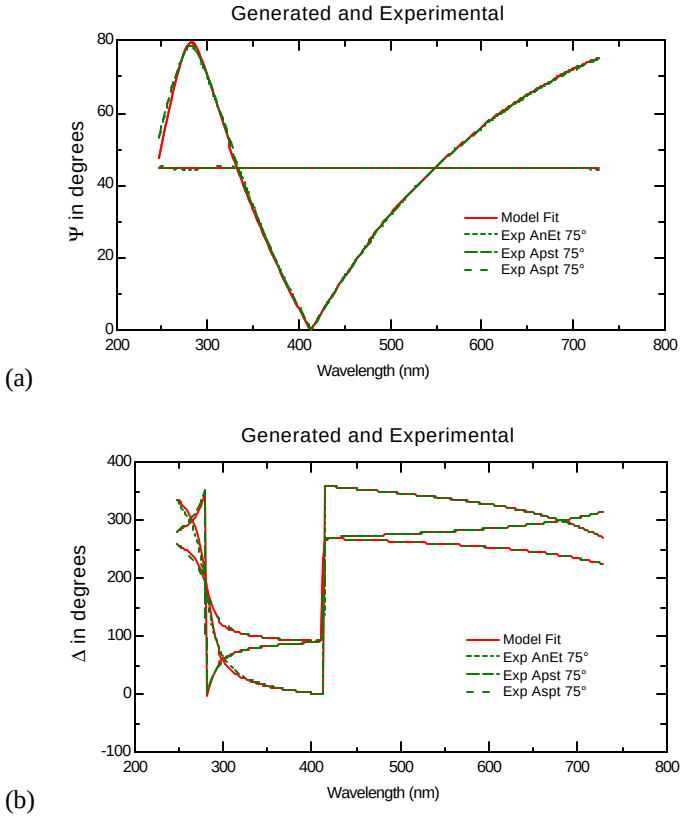

Figure 20. Generalized Spectroscopic Ellipsometric (g-SE) data acquired on a MgF_2 Berek waveplate in transmission mode, using a Diode Array Rotating Compensator Ellipsometer (DARCE)[14]. The excellent model fit to the data required only two fit parameters: the plate tip and rotation angles.

3.2. Depolarization Measurements

Another implicit assumption in the traditional ellipsometry equation (1) is that the beam reflected from the sample is totally polarized. However, if the sample depolarizes the measurement beam, the ellipsometric parameters Ψ and Δ are not well defined, and the measured 'effective' Ψ and Δ values will be dependent on the type of ellipsometer system used to acquire the data. To consider the case of a depolarizing sample requires a different formalism from the Jones matrix notation presented in the preceding section. A partially polarized beam can be quantified by a 4 element Stokes vector[46], and a 16 element Mueller matrix then completely specifies the interaction of the beam with a sample (see Equation 6). The Mueller matrix for an isotropic sample is given in Equation 7. Note that the isotropic Mueller matrix elements denoted N, C, S are defined in terms of trigonometric functions of the ellipsometric parameters Ψ and Δ. The quantity 'P', know as the degree of polarization, is defined in Equation 8 as the sum of the squares of N, C, and S; this quantity should be 1.0 for a non-depolarizing sample. If the sample depolarizes the measurement beam, the degree of polarization will be less than 1.0. Alternatively, the % depolarization can be reported, as also defined in equation 8. Even in the presence of depolarization, ellipsometric parameters Ψ and Δ can be calculated which reduce to the traditional ellipsometric values in the case of no depolarization (Equation 9). Experimentally measuring the % depolarization (or equivalently, the degree of polarization 'P') requires a compensator-based ellipsometer configuration, as the RAE and RPE configurations can not directly measure beam depolarization effects (though their effect on the RAE or RPE ellipsometric data can still be correctly accounted for in the data analysis[40]).

$$\begin{bmatrix} s_1 \\ s_2 \\ s_3 \\ s_4 \end{bmatrix}_{out} = \begin{bmatrix} m_{11} & m_{12} & m_{13} & m_{14} \\ m_{21} & m_{22} & m_{23} & m_{24} \\ m_{31} & m_{32} & m_{33} & m_{34} \\ m_{41} & m_{42} & m_{43} & m_{44} \end{bmatrix} \cdot \begin{bmatrix} s_1 \\ s_2 \\ s_3 \\ s_4 \end{bmatrix}_{in} \tag{6}$$

$$M_{isotropic} = \begin{bmatrix} 1 & -N & 0 & 0 \\ -N & 1 & 0 & 0 \\ 0 & 0 & C & S \\ 0 & 0 & -S & C \end{bmatrix} \qquad \begin{aligned} N &= \cos(2\Psi) \\ C &= \sin(2\Psi)\cdot\cos(\Delta) \\ S &= \sin(2\Psi)\cdot\sin(\Delta) \end{aligned} \tag{7}$$

$$P = N^2 + C^2 + S^2 \qquad \%\,\text{Depolarization} = 100\times(1-P) \tag{8}$$

$$\Psi = \frac{1}{2}\cdot\text{atan}\left(\frac{\sqrt{C^2+S^2}}{N}\right) \qquad \Delta = \text{atan}\left(\frac{S}{C}\right) \tag{9}$$

3.2.1. Film Thickness Non-uniformity and Spectrometer Bandwidth

Two common sources of depolarization are film thickness non-uniformity and spectrometer bandwidth (for small spot focused beam ellipsometer systems, the angle

spread of the beam is another source of depolarization). As the ellipsometric beam spot size on the sample is relatively large (1 x 4 mm is typical), it is quite possible that the film thickness is not completely uniform in this area. In this case, the interaction of various partitions of the beam with films of slightly differing thicknesses could be represented by a collection of Mueller matrices, and the net interaction of the beam with the sample over the measurement area could be modeled by a weighted average of all the corresponding Mueller matrices. % depolarization and ellipsometric parameters can be calculated from this 'net' Mueller matrix, using Equations 8 and 9. Note that since the Mueller matrix corresponding to each beam partition is of the form given in Equation 7, the net Mueller matrix is also of this form; however, the % depolarization of the net Mueller matrix is not necessarily zero. Depolarization due to finite spectrometer bandwidth can also be understood in a similar fashion, in that the collected beam contains a range of wavelengths, and a net Mueller matrix can again be found by calculating the weighted average of Mueller matrices which characterize the sample interaction vs. wavelength. In both cases, the depolarization calculation can be numerically performed in software, given an appropriate weighting function. An example of these effects is shown in Figure 21, and other examples can be found in the literature[47,48]. Depolarization caused by the backside reflection of a transparent substrate is shown in Figure 4.

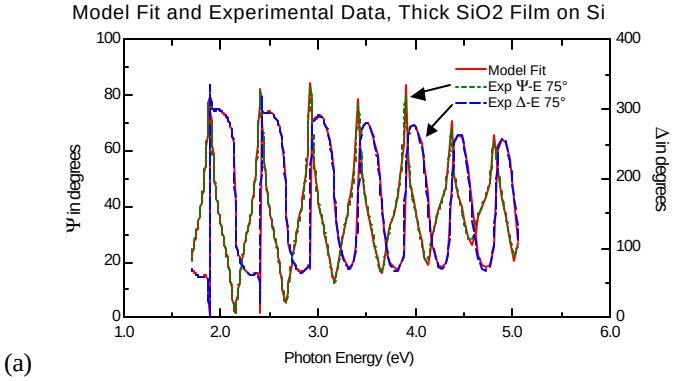

Figure 21. Spectroscopic ellipsometric (a) and depolarization (b) data acquired on a 10540Å SiO_2 film on Si by a DARCE instrument[14]. To fit the depolarization data, a spectrometer bandwidth of 7nm (assuming a Gaussian profile) and a film thickness non-uniformity of 0.44% were included in the optical model.

3.2.2. Patterned Samples

Patterned samples can also cause depolarization effects which can be readily measured and quantitatively analyzed. Actually, patterning can be simply treated as a case of film thickness non-uniformity with only a few discrete thickness values. Figure 22 shows a patterned sample in which the ellipsometric beam encompasses two regions of differing oxide thicknesses. Experimental data and the resulting model fits for such a sample are shown in Figure 23. In this analysis of this data, the native and thermal oxide thicknesses were determined (18.6±0.3Å and 998.2±0.5Å), along with the % patterned area (thermal oxide removed) covered by the measurement beam (67.5±0.1%). The patterned results were confirmed by measuring each region individually, which is also shown in the figures. As expected, the % depolarization is essentially zero for the unpatterned areas of the sample (the non-zero values below 300nm are due to stray light in the spectrometer). As patterned samples are commonplace in the manufacturing environment, the ability to quantitatively analyze data on patterned product wafers can be an enabling factor in the implementation of ellipsometric process monitoring and control (it is not desirable to dedicate wafer real estate to large metrology pads, and it is not always feasible to perform focused-beam ellipsometric measurements, for example, when performing *in situ* metrology). It should be noted that the analysis method described in this section is only valid for samples with patterning dimensions much larger than the wavelengths used in the ellipsometric measurement beam; however, an approach described by Maynard[49] may work in the very small pattern dimensions regime.

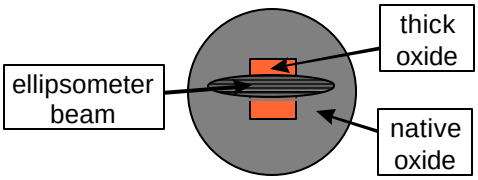

Figure 22. Schematic representation of the ellipsometric measurement of a patterned oxide sample, in which the beam overlaps native and thick oxide regions of the sample.

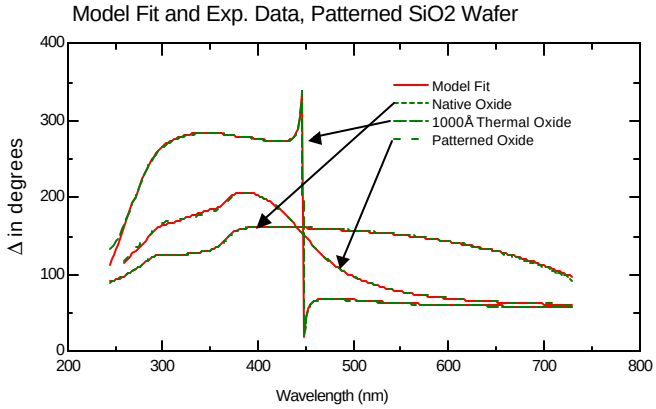

(a)

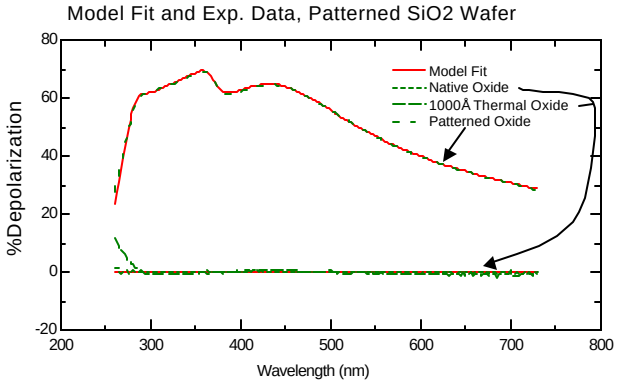

(b)

Figure 23. Spectroscopic ellipsometric (a) and depolarization (b) data acquired on a patterned SiO_2 film on Si by a DARCE instrument[14] (data measured on unpatterned native and thermal oxide areas are also shown).

3.3. Mueller Matrix Measurements

The Mueller matrix shown in Equation 6 completely specifies the specular optical response of a general sample (which may be anisotropic, depolarizing, and/or cross polarizing) at a given wavelength. Recent instrumentation[7,14,41,42] is capable of performing spectroscopic measurements of all 16 (or some subset) of the Mueller matrix elements, an example of which is shown in Figure 24. Unfortunately, the current data analysis capabilities for such measurements are essentially limited to samples which have a Mueller matrix of the form shown in Equation 7 (or its anisotropic generalization[50]). Nevertheless, Mueller matrix measurements can still be used to observe (even though they may not be quantitatively modelable) the cross polarization and scattering effects which are induced by very rough samples. Mueller matrix measurements can also be used to confirm the ideality of a sample or optical element, that is, the off-diagonal blocks of matrix elements should be zero and the m_{22} element should be 1.0.

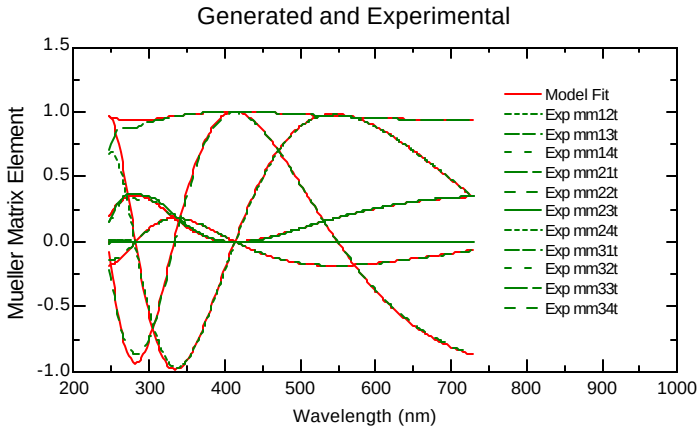

Figure 24. Mueller matrix measurement and data analysis for the MgF_2 Berek waveplate which was also measured for Figure 20. The measurement was performed with a DARCE system[14], which can measure 11 normalized (to m_{11}) Mueller matrix elements (the bottom row of the Mueller matrix is not accessible, as the compensator was placed before the sample).

4. EXTENDED SPECTRAL RANGES: FROM IR TO VUV

A strong motivation exists to measure material optical constants over increasingly broader spectral ranges. This section describes recent instrumentation advances which enable accurate measurement of ellipsometric data from the IR to VUV spectral ranges, along with examples of this powerful capability.

4.1. VASE Measurements in the IR

Fourier Transform Infra Red (FTIR) spectroscopy is a well established diagnostic technique, and in theory the advantages of ellipsometry can been applied to FTIR by adding polarizing optics to an FTIR system[51]. In practice, it is very challenging to build an accurate FTIR ellipsometer system, due to the lack of ideal optical components (both polarizers and compensators) in the IR spectral range[22]. However, by implementing a sophisticated regression calibration procedure[6] to fully characterize the non-idealities of the optical elements, and incorporating a novel IR compensator design[15], an accurate RCE FTIR system has been constructed[12,13]. This instrument can acquire VASE data over a 2 – 33 μm spectral range, with an absolute ellipsometric accuracy shown in Figures 6 and 7.

Examples of IR VASE data are shown in Figures 25 - 28. In these examples, VASE measurements in the IR are used to determine the optical constants and thickness of an IR optical coating, the doping concentration[12] and oxide thickness of a Si substrate, and IR optical constants of glass and organic materials are shown to be highly sensitive to the bonding chemistry of the material. While all of the data analysis techniques used for NIR-VIS-UV VASE data can also be applied in the IR (note the excellent model fits in Figures 25 and 26), additional analysis techniques need to be developed to quantify the rich bonding and chemistry information contained in the spectra shown in Figures 27 and 28.

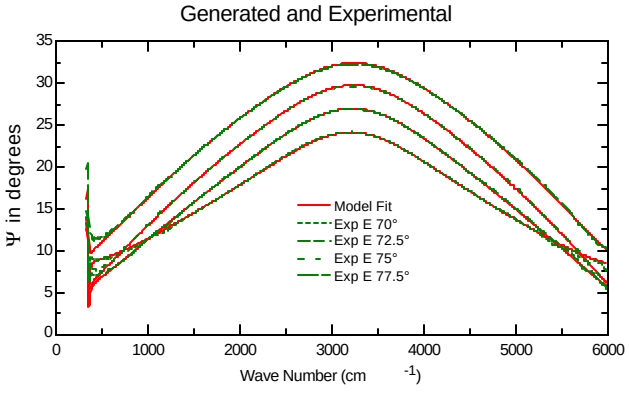

(a)

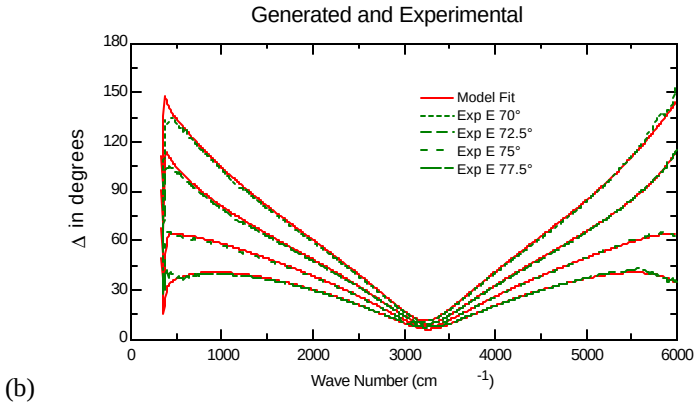

(b)

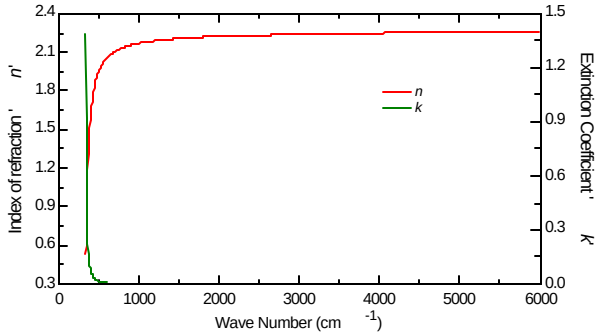

(c)

Figure 25. (a,b) IR-VASE data acquired on a 3792Å ZnS film deposited on Si. (c) resulting ZnS IR optical constants extracted from the analysis of this data.

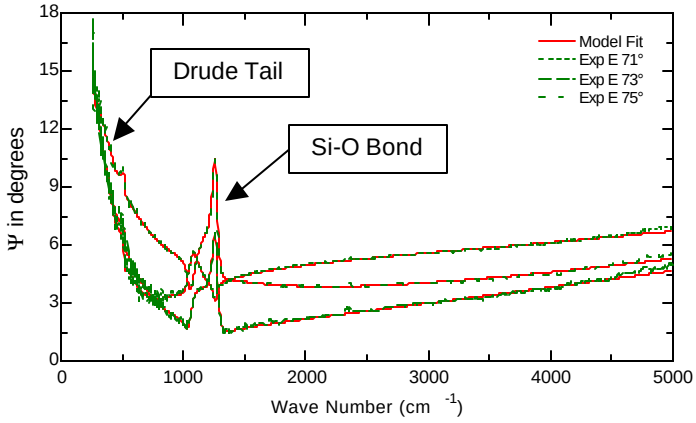

(a)

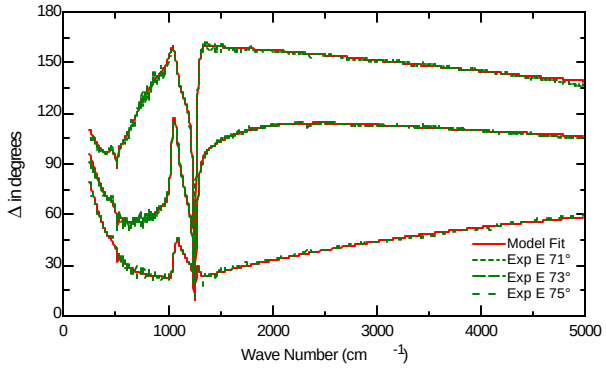

(b)

Figure 26. (a,b) IR-VASE data acquired and analyzed on a 268Å thermal oxide film on a doped Si substrate. Features due to the free carrier absorption (Drude tail) and the Si-O bond absorption are clearly seen in the data.

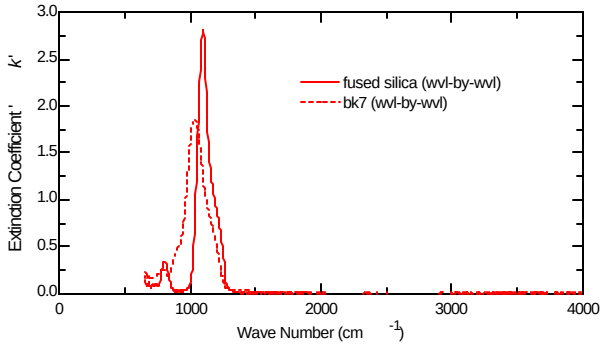

Figure 27. Extinction coefficient 'k' for bulk fused silica and BK7 glass extracted from IR-VASE data. In the visible spectral range, the optical constants for these materials are featureless and nearly the same. In IR range, the Si-O bond feature near 1000 cm^{-1} clearly differentiates these two materials.

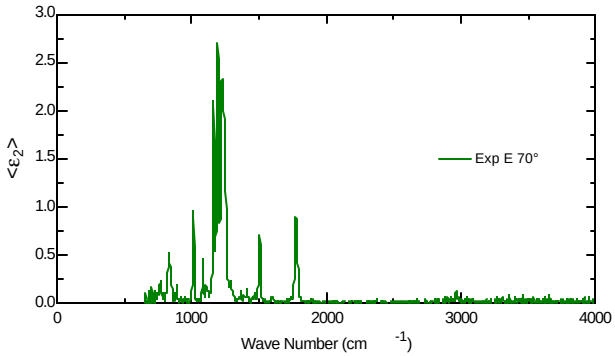

Figure 28. Imaginary part of the dielectric function, ε_2, directly extracted from the IR-VASE measurement of a bulk polycarbonate sample. The RCE configuration of the instrument enabled the accurate measurement of the low ε_2 values in this spectral range, as the ellipsometric Δ parameter is essentially zero for most of this data set. Note the abundance of sharp IR absorption bands, which is typical of most organic materials, and may be used to directly characterize the chemistry of the material.

4.2. VUV Ellipsometry

A RAE system equipped with an adjustable retarder[7] has been operated in the UV-VUV spectral range (4.2 – 8.5 eV, or 146 – 300 nm). To achieve operation in this spectral range, a deuterium lamp coupled with a scanning monochromator was used as a light source, along with MgF_2 optics. Examples of spectroscopic ellipsometric data acquired with this system are shown in Figure 29, and in section 2.2 of this paper. As the next targeted lithography line is 157nm, there is a tremendous demand for optical constant measurements in this VUV spectral range of materials used in Si-based semiconductor technology (especially photoresists), and of optical elements (and coatings) used in lithographic stepper equipment. Wide band-gap materials such as $Al_xGa_{1-x}N$ (which is used in blue LEDs and lasers) will also benefit from VASE characterization in the VUV spectral range[53].

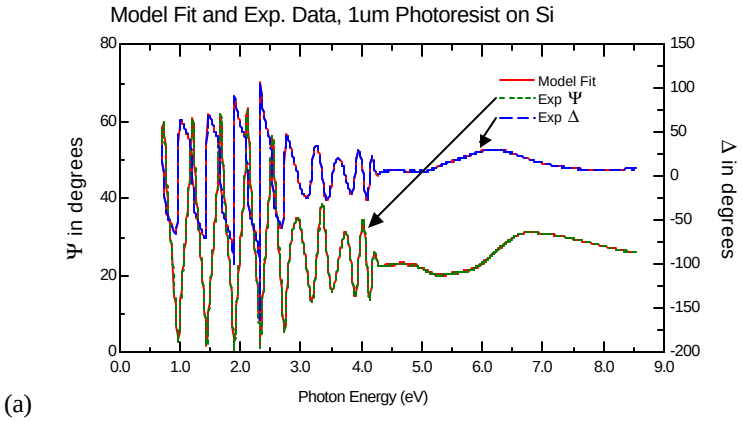

(a)

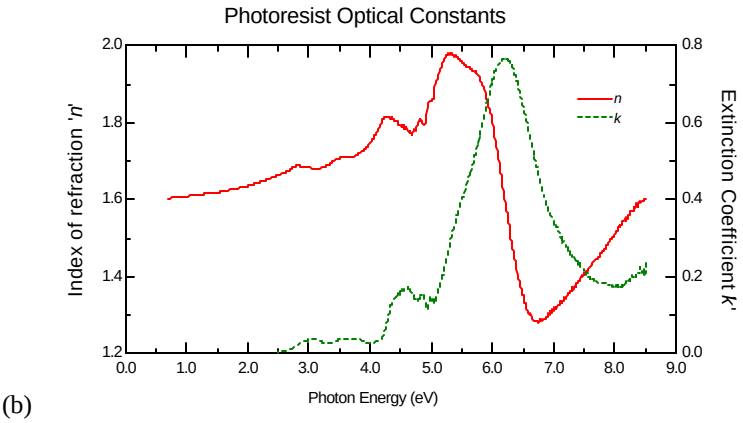

(b)

Figure 29. (a) UV-VUV spectroscopic ellipsometric data from a≈1 µm photoresist film on Si; NIV-VIS-UV data acquired on a different instrument is also appended to the curve. (b) Photoresist optical constants resulting from an analysis of the data, using the Si substrate optical constants shown in Figure 15.

SUMMARY

Advanced instrumentation which can acquire extremely accurate VASE data, generalized ellipsometry data, depolarization and Mueller matrix data over a broad spectral range (IR to VUV) has greatly enhanced the material characterization capabilities of the VASE technique, as illustrated by the many applications in this paper. The accuracy of the measured data and the validity of the optical models used in the data analysis were confirmed by the near perfect data fits which were achieved in these applications. Powerful data analysis techniques such as GBPS parameterization and multi-sample analysis were also shown to be extremely useful in extracting material properties (optical constants and structural parameters) from the wide spectral range measurements.

ACKNOWLEDGMENTS

The authors wish to thank the many sponsors who contributed to the development of the work presented here, including NASA, BMDO, the U.S. Army and Air Force, DARPA, and numerous corporations which supplied samples.

REFERENCES

1. P.S. Hauge, “Recent developments in instrumentation in ellipsometry”, Surf. Sci. 96, 108 (1980).
2. R.W.Collins, “Automatic rotating element ellipsometers: Calibration, Operation, and Real-time Applications”, Rev.Sci.Instrum. 61, 2029 (1990).
3. J.M.M. de Nijs and A. van Silfhout, “Systematic and random errors in rotating-analyzer ellipsometry”, J. Opt. Soc. Am. A. 5, 773 (1988).
4. B. Drevillon, J. Perrin , R. Marbot, A. Violet, and J.L. Dalby, Rev. Sci. Instrum. 53, 969 (1982).
5. G.E. Jellison Jr. and F.A. Modine, “A two -channel polarization modulation ellipsometer”, Appl. Opt. 29, 959 (1990).
6. B. Johs, “Regression calibration method for rotating element ellipsometers”, Thin Solid Fillms 234, 395 (1993).
7. VASE system with AutoRetarder option, J.A. Woollam Co., Inc., Lincoln, NE USA.
8. US Patent #5,757,494, “System and method for improving data acquisition capability in spectroscopic ellipsometers”.
9. R. Kleim, L. Kuntzler, and A. El Ghemmaz, “Systematic errors in rotating compensator ellipsometry”, J. Opt. Soc. Am. A 11, 2550 (1994).
10. J. Lee, P.I. Rovira, I. An, and R.W. Collins, "Rotating compensator multichannel ellipsometry: applications for real time Stokes vector spectroscopy of thin film growth", Rev. Sci. Instrum. 69, 1800-1810 (1998).
11. J. Opsal, J. Fanton, J. Chen, J. Leng, L. Wei, C. Uhrich, M. Senko, C. Zaiser, D.E. Aspnes, “Broadband spectral operation of a rotating-compensator ellipsometer”, Thin Solid Films 313-314, 58 (1998).
12. T.E. Tiwald, D.W. Thompson, J.A. Woollam, W. Paulson, and R. Hance, “Application of IR variable angle spectroscopic ellipsometry to the determination of free carrier concentration depth profiles”, Thin Solid Films 313-314, 661 (1998).
13. IR-VASE system, J.A. Woollam Co., Inc., Lincoln, NE USA.
14. M-2000 ellipsometer system, J.A. Woollam Co., Inc., Lincoln, NE USA.
15. US Patent #5,706,212, “Infrared ellipsometer/polarimeter system, method of calibration, and use thereof”.

16. US Patent #5,872,630, “Regression calibrated spectroscopic rotating compensator ellipsometer system with photo array detector”.
17. R.W. Collins, I. An, H. Fujiwara, J. Lee, Y. Lu, J. Koh, and P.I. Rovira, “Advances in multichannel spectroscopic ellipsometry”, Thin Solid Films 313-314, 18 (1998).
18. R.A. Synowicki, “Spectroscopic ellipsometry characterization of indium tin oxide film microstructure and optical constants”, Thin Solid Films 313-314, 394 (1998).
19. T. Yasuda and D.E. Aspnes, “Optical-standard surfaces of single-crystal silicon for calibrating ellipsometers and reflectometers”, Applied Optics 33, 7435 (1994).
20. G.E. Jellison Jr., “Examination of thin SiO_2 films on Si using spectroscopic polarization modulation ellipsometry”, J. Appl. Phys. 69, 7627 (1991).
21. C.M. Herzinger, B. Johs, W.A. McGahan, J.A. Woollam, and W. Paulson, “Ellipsometric determination of optical constants for silicon and thermally grown silicon dioxide via a multi-sample, multi-wavelength, multi-angle investigation”, J. Appl. Phys. 83, 3323 (1998).
22. M. Luttmann, J-L Stehle, C. Defranoux, and J-P Piel, “High accuracy IR ellipsometer working with a Ge brewster angle reflection polarizer and grid analyzer”, Thin Solid Films 313-314, 631 (1998).
23. G.E. Jellison Jr., “Data analysis for spectroscopic ellipsometry”, Thin Solid Films 234, 416 (1993).
24. F. Wooten, Optical Properties of Solids, Academic press, New York, 1972.
25. F. Terry Jr., “A modified harmonic oscillator approximation scheme for the dielectric constants of $Al_xGa_{1-x}As$,” J. Appl. Phys. 70, 409 (1991).
26. G.E. Jellison Jr. and F.A. Modine, “Parameterization of the optical functions of amorphous materials in the interband region”, Appl. Phys. Lett. 69, 371 (1996).
27. C.C. Kim, J.W. Garland, H. Abad, and P.M. Raccah, “Modeling the optical dielectric function of semiconductors: extension of the critical-point parabolic-band approximation,” Phys. Rev. B 45, 11749 (1992).
28. S. Zollner, “Model dielectric function for native oxides on compound semiconductors,” Appl. Phys. Lett. 63, 2523 (1993).
29. J. Leng, J. Opsal, H. Chu, M. Senko, and D.E. Aspnes, “Analytic representations of the dielectric functions of materials for device and structural modeling”, Thin Solid Films 313-314, 132 (1998).
30. US Patent #5,796,983, “Dielectric function parametric model, and method of use”.
31. B. Johs, C.M. Herzinger, J.H. Dinan, A. Cornfeld, and J.D. Benson, “Development of a parametric optical constant model for $Hg_{1-x}Cd_xTe$ for control fo composition by spectroscopic ellipsometry during MBE growth.
32. H.G. Tompkins, A User’s Guide to Ellipsometry, Academic Press (1993).
33. C.M. Herzinger, H. Yao, P.G. Synder, F.G. Celii, Y.-C. Kao, B. Johs, and J.A. Woollam, “Determination of AlAs optical constants by variable angle spectroscopic ellipsometry and an multisample analysis”, J. Appl. Phys. 77, 4677 (1995).
34. W.A. McGahan, B. Johs, and J.A. Woollam, “Techniques for ellipsometric measurement of the thickness and optical constants of thin absorbing films”, Thin Solid Films 234, 443 (1993).
35. D.E. Aspnes and A.A. Studna, Phys. Rev. B 26, 7466 (1983).
36. G.E. Jellison Jr., Opt. Mater. 1, 41 (1992).
37. R.M.A. Azzam and N.M Bashara, “Generalized ellipsometry for surfaces with directional preference: application to diffraction gratings”, J. Opt. Soc. Am. 62, 883 (1972).
38. M. Schubert, “Generalized ellipsometry and complex optical systems”, Thin Solid Films 313-314, 323 (1998).
39. A R✱seler, “Problem of polarization degree in spectroscopic photometric ellipsometry (polarimetry)”, J. Opt. Soc. Am. A 9, 1124 (1992).
40. K. Forcht, A. Gombert, R. Joerger, M. K✱hl, “Incoherent superposition in ellipsometric measurements”, Thin Solid Films 302, 43 (1997).
41. R.W. Collins and J. Koh, "Dual rotating compensator multichannel ellipsometer: instrument design for real time Mueller matrix spectroscopy of surfaces and films" J. Opt. Soc. Am. A 16 (in press, August 1999).

42. G.E. Jellison Jr., F.A. Modine, and L.A. Boatner, "The measurement of the optical functions of uniaxial materials using two -modulator generalized ellipsometry: Rutile (TiO_2)", Opt. Lett. 22, 1808 (1997).
43. M. Schubert, B. Rheinl•nder, J.A. Woollam, B. Johs, and C.M. Herzinger, "Extension of rotating-analyzer ellipsometry to generalized ellipsometry: determination of the dielectric function tensor from uniaxial TiO_2", J. Opt. Soc. Amer. A 13, 876 (1996).
44. J.F. Elman, J. Greener, C.M. Herzinger, and B. Johs, "Characterization of biaxially-stretched plastic films by generalized ellipsometry", Thin Solid Films 313-314, 814 (1998).
45. M. Schubert, "Polarization-dependent optical parameters of arbitrarily anisotropic homogeneous layered systems", Phys. Rev. B 53, 4265 (1996).
46. R.M.A. Azzam, and N.M.Bashara, Ellipsometry and Polarized Light, North Holland Press, Amsterdam 1977, Second edition 1987.
47. G.E. Jellison Jr. and J.W. McCamy, "Sample depolarization effects from thin films of ZnS on GaAs as measured by spectroscopic ellipsometry", Appl. Phys. Lett. 61, 512 (1992).
48. U. Richter, "Application of the degree of polarization to film thickness gradients", Thin Solid Films 313-314, 102 (1998).
49. H.L. Maynard, N. Layadi, J.T.C. Lee, "Plasma etching of submicron devices : in situ monitoring and control by multi-wavelength ellipsometry", Thin Solid Films 313-314, 398 (1998).
50. G.E. Jellison Jr., "Spectroscopic ellipsometry data analysis: measured versus calculated quantities", Thin Solid Films 313-314, 33 (1998).
51. A. R✱seler, Infrared Spectroscopic Ellipsometry, Akademie-Verlag, Berlin, 1990.
52. C.M. Herzinger, B. Johs, W.A. McGahan, W. Paulson, "A multi-sample, multi-wavelength, multi-angle investigation of the interface layer between silicon and thermally grown silicon dioxide", Thin Solid Films 313-314, 281 (1998).
53. T. Wethkamp, K. Wilmers, N. Esser, W. Richter, O. Ambacher, H. Angerer, G. Jungk, R.L. Johnson, M. Cardona, "Spectroscopic elliposmetry measurements of $Al_xGa_{1-x}N$ in the energy range 3-25 eV", Thin Solid Films 313-314, 745 (1998).